Aven blocks DNA damage-induced apoptosis by stabilising Bcl-xL

Ozgur Kutuk [a], Sehime Gulsun Temel [b], Sahsine Tolunay [c], Huveyda Basaga [a,*]

[a] Biological Sciences and Bioengineering Program, Faculty of Natural Sciences and Engineering, Sabanci University, 34956, Tuzla, Istanbul, Turkey
[b] Department of Medical Genetics, Faculty of Medicine, Uludag University, Bursa, Turkey
[c] Department of Pathology, Faculty of Medicine, Uludag University, Bursa, Turkey

ARTICLE INFO

ABSTRACT

Induction of apoptosis by DNA-damaging agents involves the activation of mitochondrial apoptotic pathway. Aven has been identified as an antiapoptotic protein and has been shown to activate ATM in response to DNA damage. In this study, we demonstrated that enforced expression of Aven blocks UV-irradiation-, SN-38- or cisplatin-induced apoptosis upstream of mitochondria by stabilising Bcl-xL protein levels in breast cancer cells. Aven silencing by RNA interference markedly enhanced apoptotic response following treatment with DNA-damaging agents. Aven is complexed with Bcl-xL in untreated breast cancer cells and treatment with DNA-damaging agents led to decreased Aven/Bcl-xL interaction. Importantly, Bcl-xL was necessary for the prosurvival activity of Aven and depletion of Bcl-xL abrogated Aven-mediated protection against DNA damage-induced apoptosis. Analysis of breast cancer tissue microarrays revealed decreased Aven nuclear expression in breast cancer tissues compared with non-neoplastic breast tissues. In particular, we detected reduced nuclear expression of Aven in infiltrating ductal carcinoma and papillary carcinoma breast cancer subtypes compared with non-neoplastic breast tissues and infiltrating lobular breast cancer tissues. Our results suggest that Aven is an important mediator in DNA damage-induced apoptotic signalling in breast cancer cells and its nuclear expression is altered in breast cancer tissues, which may contribute to genomic instability in breast cancer tumours.

© 2010 Elsevier Ltd. All rights reserved.

1. Introduction

Cells respond to DNA damage by activating cell cycle checkpoints and DNA repair mechanisms or by engaging prodeath pathways.[1,2] Genotoxic chemotherapeutic drugs and irradiation target DNA to activate mitochondrial apoptotic pathway in cancer cells. Deregulation of DNA damage-induced apoptosis promotes tumourigenesis[3–5] and may lead to emergence of chemoresistance.[6–9] Therefore, it is vital to identify the mechanisms of resistance to DNA damage-induced apoptosis and to target these mechanisms for increasing the effectiveness of cancer therapy.

Activation and oligomerisation of Bax and Bak mediate mitochondrial outer membrane permeabilisation (MOMP) and the release of cytochrome c into cytosol following proapoptotic insults, such as growth factor withdrawal, anoxia and genotoxic stress.[10–14] When released into the cytosol, cytochrome c binds to Apaf-1, triggers the formation of

apoptosome and caspase activation.[15] Prosurvival Bcl-2 protein family members (Bcl-2, Bcl-xL, Mcl-1, Bcl-w and Bfl-1) prevent MOMP either by sequestering sensitiser BH3-only proteins (Bad, Puma, Bmf, Noxa and Bik) or by directly binding and inhibiting Bax and Bak.[16–19] Recent studies demonstrated that development of targeted therapeutics against prosurvival Bcl-2 proteins is a rational approach to eliminate chemoresistant cancer cells in various cancer types when used in combination with chemotherapeutics.[20–22] Importantly, increased expression of Bcl-xL, Bcl-2 or Mcl-1 has been shown to confer resistance to chemotherapy and to be associated with poor prognosis in breast cancer.[23–26] Of note, National Cancer Institute's *in vitro* anticancer drug screen has also identified a strong negative correlation between drug sensitivity and Bcl-xL levels, although such a correlation could not be detected for Bax or Bcl-2.[27]

Aven has been identified as an antiapoptotic protein that interacts with Bcl-xL and Apaf-1.[28] The prosurvival effect of Aven can be attributed to the ability of Aven to potentiate Bcl-xL antiapoptotic activity or to inhibit Apaf-1 proapoptotic function. Recently, Aven was also shown to directly interact and activate ATM kinase, thereby acts as a critical regulator of G2/M DNA damage checkpoint.[29] Overexpression of Aven in *Xenopus leavis* egg extracts led to cell cycle arrest and knockdown of Aven resulted in the decreased activation of ATM in response to DNA damage. In addition, ATM can also phosphorylate Aven at Ser135 and Ser138, which is required for Aven-induced cell cycle arrest.[29]

Here we tested the role of Aven in the regulation of DNA damage-induced apoptosis in breast cancer cells. We demonstrated that Aven inhibits DNA damage-induced apoptosis by stabilising Bcl-xL protein levels and Bcl-xL is essential for the prosurvival activity of Aven. We also investigated the expression profile of Aven in primary breast cancer tissues using tissue microarrays (TMAs). Our data showed diminished Aven nuclear expression in breast cancer tissues compared with non-neoplastic breast tissues. We also demonstrated decreased Aven nuclear expression in infiltrating ductal carcinoma and papillary carcinoma breast cancer subtypes compared with non-neoplastic breast tissues and infiltrating lobular cancer tissues.

These findings provide a plausible mechanism that Aven may confer resistance to DNA damage-induced apoptosis in breast cancer cells and support the need for further studies to illustrate the contribution of Aven to clinical outcome in breast cancer.

2. Materials and methods

2.1. Cell lines and reagents

ZR-75-1, BT20, BT549 and MDA-MB-468 cells were grown in RPMI 1640 (Biological Industries, Beit-Haemek, Israel) with 2 mM L-glutamine, 10% foetal calf serum, 100 IU/ml penicillin and 100 μg/ml streptomycin in a humidified incubator at 37 °C and 5% CO_2. MDA-MB-468, BT20, BT549 and ZR-75-1 cells were transfected either with empty vector (pSG5 Vector) or with pSG5 HA-Aven using Fugene 6 (Roche, Mannheim, Germany). The expression levels of Aven and HA-Aven in parental, vec-

tor-transfected and HA-Aven-transfected cells were verified by using immunoblotting using anti-Aven and anti-HA antibodies.

SN-38, cisplatin and cycloheximide were purchased from Sigma–Aldrich (St. Louis, MO). Stratalinker 2400 (Stratagene, La Jolla, CA) was used for UV-irradiation.

2.2. Apoptosis assays

Apoptosis was evaluated as levels of specifically DEVDase-cleaved cytokeratin-18 in total cell lysates by using M30 Apoptosense assay (PEVIVA AB, Bromma, Sweden) as described before[30] and results were presented as fold increase in units per litre. Apoptosis was also detected by using Annexin V-FLUOS Staining Kit (Roche, Mannheim, Germany) and flow cytometry. The activities of caspase-9, caspase-3 and caspase-8 were determined by ApoAlert Caspase Profiling Plate (Clontech, Palo Alto, CA) according to the manufacturer's protocol. The release of fluorochrome7-amino-4-methyl coumarin was analysed at 380-nm excitation and 460-nm emission using a multiplate fluorescence spectrophotometer. Data shown are means ± SEM of three independent experiments in duplicate and expressed in arbitrary fluorescence units per mg of protein.

2.3. Immunoblot analysis

Total cell lysates were prepared in 1% CHAPS buffer (5 mM $MgCl_2$, 137 mM NaCl, 1 mM EDTA, 1 mM EGTA, 1% Chaps (w/v), 20 mM Tris–HCl (pH 7.5) and protease inhibitors (Roche, Mannheim, Germany). Proteins were separated on SDS gel electrophoresis and transferred onto PVDF membranes (GE Healthcare, Little Chalfont, UK). Membranes were blocked with 5% milk blocking solution (w/v) in PBS-Tween20 and incubated with primary and HRP-conjugated secondary antibodies in a buffer containing 10% milk diluent concentrate (KPL, USA). Proteins were finally analysed by using ECL Advance chemiluminescence (GE Healthcare, Little Chalfont, UK) and exposing membranes to Hyperfilm ECL (GE Healthcare, Little Chalfont, UK). The following antibodies were used for immunoblotting: anti-Aven (BD Biosciences, San Diego, CA), anti-HA (Abcam, Cambridge, UK), anti-Actin, anti-Bcl-xL, anti-Bcl-2 and anti-Mcl-1 (Cell Signaling Technology, Beverly, MA).

2.4. Coimmunoprecipitation

Cell lysates were isolated in 1% Chaps buffer as described previously.[31] Briefly, total proteins (800 μg) were immunoprecipitated with anti-Aven (BD Biosciences, San Diego, CA) and anti-Bcl-xL (Cell Signaling Technology, Beverly, MA) antibodies at 4 °C for 2 h or overnight. Immunoprecipitates were captured by 50% slurry of protein G-Sepharose (GE Healthcare, Little Chalfont, UK) in lysis buffer at 4 °C for 2 h. Immunoprecipitates were then recovered by centrifugation and washed three times in 1% Chaps buffer. The samples were subsequently analysed by immunoblot to detect interacting proteins.

2.5. *Assessment of Bax and Bak activation*

Detection of Bax and Bak activation by intracellular staining and flow cytometry using active conformation-specific antibodies anti-Bax (6A7, BD Pharmingen) and anti-Bak (Ab-1, Calbiochem) was performed as described previously.[32] Activation of Bax or Bak was determined by a shift to the right in the histogram.
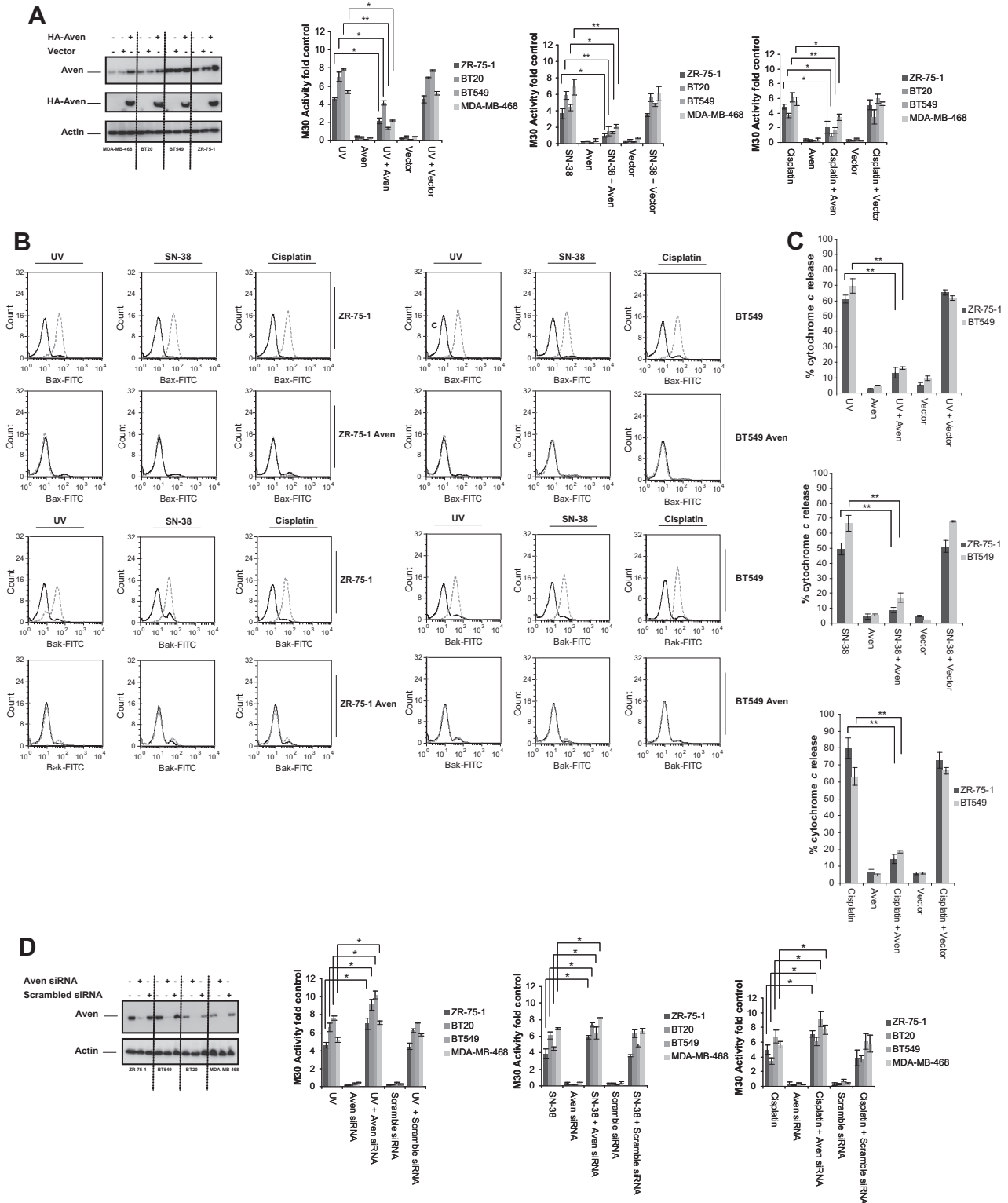
2.6. Assessment of cytochrome c release

The mitochondrial release of cytochrome *c* was assayed by using Chemicon cytochrome *c* ELISA kit (Millipore, Bedford, MA) according to the manufacturer's protocol. Results are expressed as percent cytochrome *c* release compared with control (means ± SEM, $n = 4$).

2.7. Small interfering RNA transfection

MDA-MB-468, BT20, BT549 and ZR-75-1 cells were transfected with Aven siRNA Hs_AVEN_5 HP Validated siRNA, Qiagen, Hilden, Germany), Bcl-xL siRNA Hs_BCL2L1_8 HP siRNA, Qiagen, Hilden, Germany) or Scrambled siRNA (Negative Control siRNA, Qiagen, Hilden, Germany) by using Hiperfect transfection reagent (Qiagen, Hilden, Germany) according to the manufacturer's instructions. The efficiency of protein knockdowns was verified by immunoblotting.

2.8. Measurement of Bcl-xL, Bcl-2 and Mcl-1 Half-life

Cycloheximide (10 µg/ml) was added to ZR-75-1 and BT549 cells 24 h after transfection with pSG5 HA-Aven. Similarly, cells were treated with cycloheximide (10 µg/ml) 48 h after treatment with Aven siRNA. Cell lysates were isolated at the indicated time points and the expression levels of Bcl-xL, Mcl-1 and Bcl-2 were determined by immunoblotting. For Bcl-xL, protein expression levels were semi-quantitatively determined by densitometry using ImageJ 1.41 software (ImageJ, NIH, USA) and expressed as a ratio of Bcl-xL/Actin.

2.9. Tissue microarrays and immunohistochemistry

Aven protein expression and localisation were assessed on tissue microarrays (TMA) containing normal and malignant breast tissues. Tissue microarrays (A202-III, A202-IV, ISU AB-XIS, Seoul, Korea) were deparaffinised with xylol, passed through graded alcohols and rinsed successively in distilled water. This treatment was followed by the use of 1% hydrogen peroxide in order to block the endogenous peroxidase and then the sections were washed and processed for the antigen

retrieval procedure in 10 mM citrate buffer (pH 6.0) in a microwave oven. Following blocking in normal horse serum (10% in Tris–HCl buffer containing 0.1% sodium azide and 0.2% Triton X-100), sections were incubated with the primary antibody (mouse monoclonal anti-Aven, 1:300, BD Biosciences) for 4 h at room temperature. The sections were then incubated for 60 min in the affinity-purified biotin-conjugated donkey anti-mouse antibody (1:250, Jackson Immunoresearch Labs, West Grove, PA). Next, sections were processed for bright field immunohistochemistry using the Elite ABC Kit (Vector Labs, Burlingame, CA) according to the instructions of the manufacturer. In order to visualise the antigen-antibody complex, diamino benzidine (DAB) was used as the chromogen. Positively stained cells were counted in up to five different areas, and the frequency of positive cells was determined in percentage. Scoring was done by taking into account both the intensity of staining and the distribution of positively stained cells. The intensity and distribution pattern of protein expression were evaluated by two independent observers, neither of whom had access to the diagnosis, by using a semi-quantitative method (immunoreactive score (IRS)) as previously described.[33] Briefly, the IRS was calculated by multiplication of staining intensity (graded as 0: none, 1: weak, 2: moderate and 3: strong staining) and the percentage of positive staining cells (0: no stained cells, 1: <10% of the cells, 2: 11–50% of the cells, 3: 51–80% of the cells and 4: >81% of the cells).

2.10. Statistical analysis

GraphPad Prism 3.0 software (Graphpad Software, San Diego, CA, USA) and SPSS/PC software package version 13.0 (SPPS, Chicago, USA) were used for statistical data analysis. Student's *t*-tail, Mann–Whitney *U* and Kruskal–Wallis tests were used for comparison of data; significance was set at *$p < 0.05$ and **$p < 0.01$.

3. Results and discussion

Aven was demonstrated to increase the survival of CD-1 mice infected with Sindbis virus.[28] In addition, the protective effect

Fig. 1 – Aven blocks DNA-damage-induced apoptosis upstream of mitochondrial apoptotic pathway. (A) MDA-MB-468, BT20, BT549 and ZR-75-1 cells were transfected either with empty vector (pSG5 Vector) or with pSG5 HA-Aven. After 48 h, total cell lysates were prepared and the expression level of Aven and HA-Aven in parental, vector-transfected and HA-Aven-transfected cells was verified by using immunoblotting using anti-Aven and anti-HA antibodies. Cells were exposed to UV (80 mJ/cm²) or treated with SN-38 (60 nM) and cisplatin (20 µM). Apoptosis was evaluated by M30 Apoptosense assay after 48 h (mean ± SEM, $n = 4$, *$p < 0.05$, **$p < 0.01$ by two-tailed *t*-test). (B) ZR-75-1, pSG5 HA-Aven-transfected ZR-75-1 (ZR-75-1 Aven), BT549 and pSG5 HA-Aven-transfected BT549 (BT549 Aven) cells were exposed to UV (80 mJ/cm²) or treated with SN-38 (60 nM) and cisplatin (20 µM). Cells were stained for active conformation-specific Bax (6A7) or Bak (Ab-1) after 12 h, followed by incubation with FITC-conjugated secondary antibody. Active Bax- or active Bak-related immunofluorescence was analysed by flow cytometry. *Black line,* control cells; *grey dots,* treated cells. (C) ZR-75-1, ZR-75-1 Aven, BT549 and BT549 Aven cells were exposed to UV (80 mJ/cm²) or treated with SN-38 (60 nM) and cisplatin (20 µM). The mitochondrial release of cytochrome *c* was evaluated by using an ELISA-based assay (means ± SEM, $n = 4$, **$p < 0.01$ by two-tailed *t*-test). (D) ZR-75-1, BT549, MDA-MB-468 and BT20 cells were treated with Aven siRNA or Scrambled siRNA for 48 h followed by UV-irradiation (80 mJ/cm²) or treatment with SN-38 (60 nM) and cisplatin (20 µM). The efficiency of Aven knockdown was checked by immunoblots. Apoptosis was evaluated 48 h after exposure to UV, SN-38 or cisplatin by M30 Apoptosense assay (mean ± SEM, $n = 4$, *$p < 0.05$ by two-tailed *t*-test).

of Aven has been observed in IL-3-deprived and γ-irradiated FL5.12 cells,[28] which suggests that Aven provides protection against diverse prodeath stimuli in cells. Similarly, Aven was reported to act synergistically with Bcl-xL to decrease cell

death following serum deprivation or staurosporine treatment in Chinese hamster ovary cells.[34] To test whether Aven overexpression in breast cancer cells protects against DNA damage-induced apoptosis, ZR-75-1, BT20, BT549 and MDA-MB-468
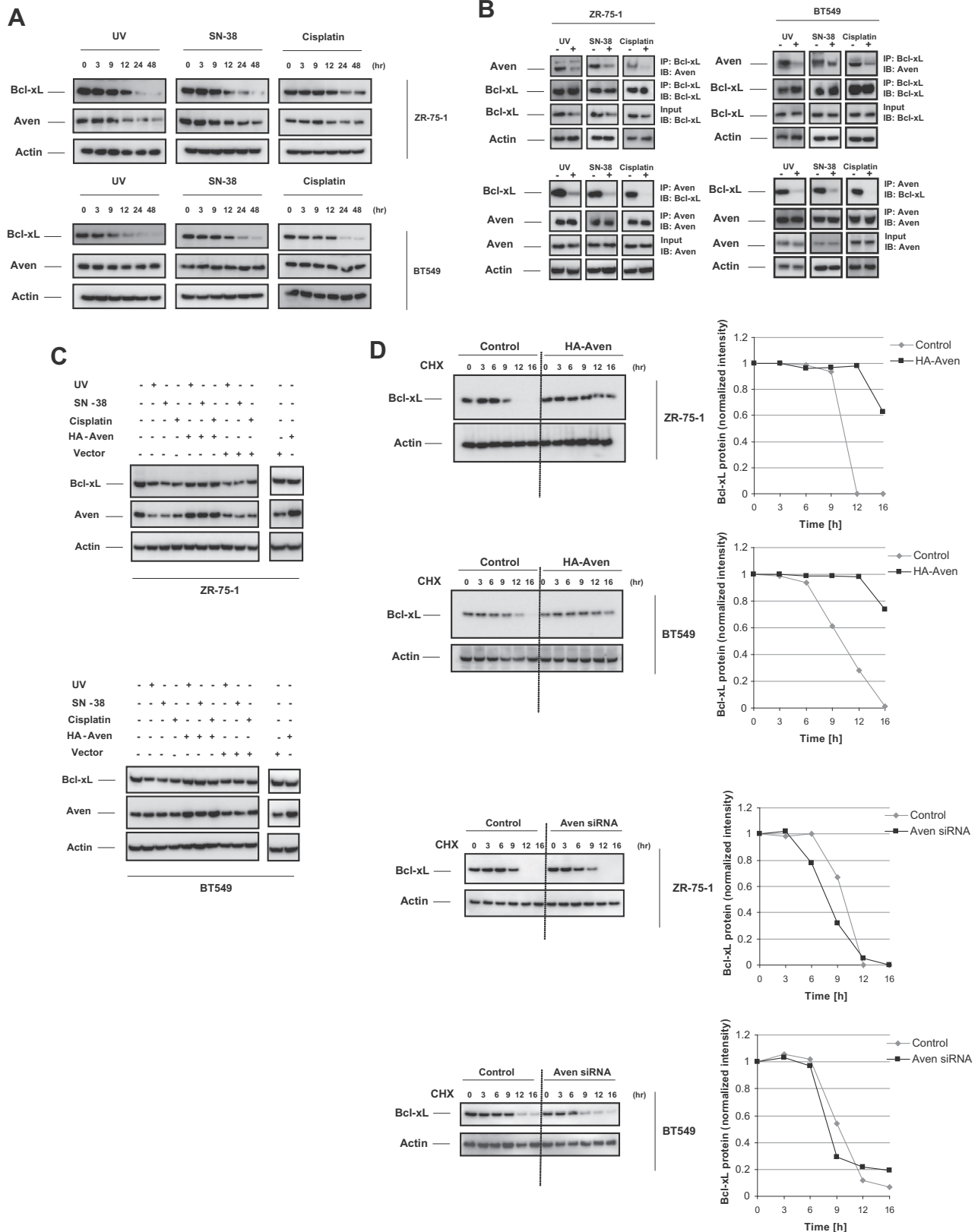
cells were transfected either with empty vector (pSG5 Vector) or with pSG5 HA(haemagglutinin)-Aven. We verified the expression level of Aven protein in untransfected and transfected cells by immunoblotting (Fig. 1A). Cells were subjected to UV damage or treated with SN-38 (an active metabolite of irinotecan) or cisplatin and apoptosis was determined by using M30 Apoptosense ELISA assay. As shown in Fig. 1A, over-expression of Aven in ZR-75-1, BT20, BT549 and MDA-MB-468 cells significantly decreased apoptosis induction by UV, SN-38 or cisplatin treatment. Annexin V staining assays also confirmed the protective effect of Aven against UV-, SN-38- or cisplatin-induced cell death in breast cancer cells (Fig. S4A). Next, we asked whether Aven suppresses apoptosis upstream of mitochondrial permeabilisation by inhibiting Bax and Bak activation. We tested the activation of Bax and Bak by employing conformation-specific antibodies for immunofluorescence staining and flow cytometry detection. Our results show that overexpression of Aven in BT549 and ZR-75-1 cells prevented Bax and Bak activation by UV exposure and SN-38 or cisplatin treatment (Fig. 1B). Consistent with this observation, enforced expression of Aven inhibited the release of cytochrome c into cytosol in response to UV, SN-38 or cisplatin treatment in BT549 and ZR-75-1 cells as determined by cytochrome c ELISA assays (Fig. 1C). Inhibition of DNA damage-induced apoptosis by Aven was also confirmed by fluorometric caspase assays. Aven overexpression inhibited activation of caspase-3 and caspase-9 in response to treatment with UV-irradiation, cisplatin and SN-38, whereas caspase-8 activity was not altered (Figs. S1A, S2A and S3A).

To evaluate the role of endogenous Aven expression in the apoptotic response to DNA damage-induced apoptosis, we employed knockdown experiments with Aven siRNA or Scrambled siRNA and exposed ZR-75-1, BT20, BT549 and MDA-MB-468 cells to UV, SN-38 or cisplatin. We confirmed the efficiency of Aven depletion by RNA interference using immunoblotting (Fig. 1D). M30 Apoptosense ELISA assays demonstrated increased apoptosis in Aven siRNA-treated breast cancer cells upon treatment with UV, SN-38 or cisplatin, compared with control cells. These findings were also confirmed by using Annexin V staining and flow cytometry analysis (Fig. S4B). Scrambled siRNA did not show any significant effect on DNA damage-induced cell death. Moreover, depletion of Aven by siRNA resulted in enhanced activation
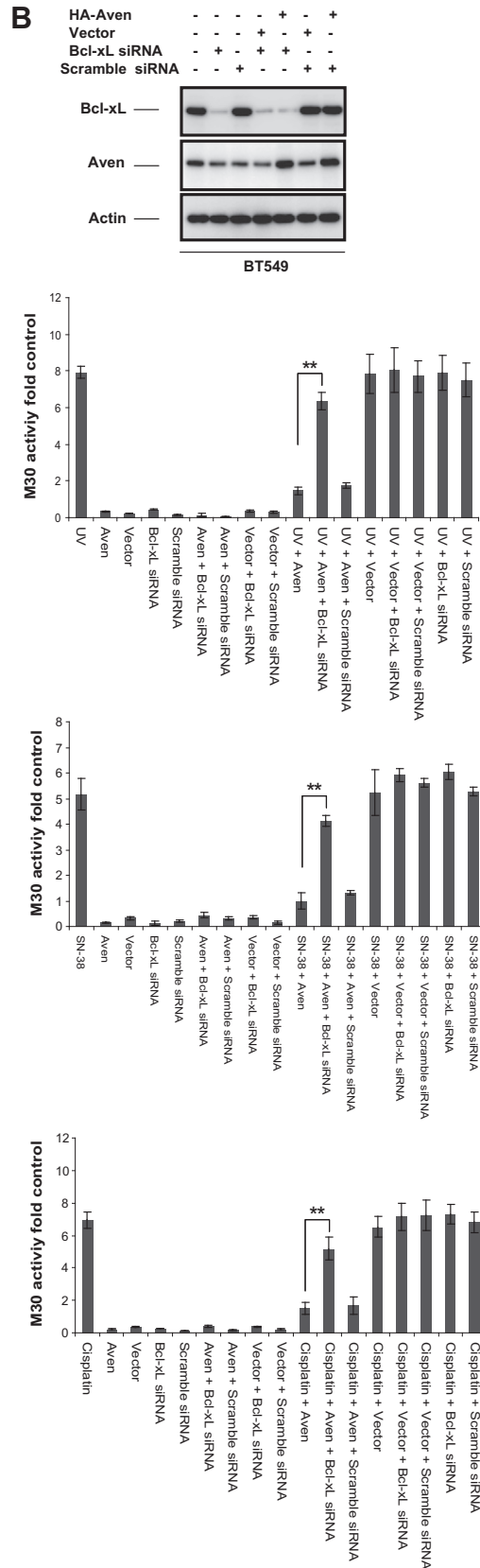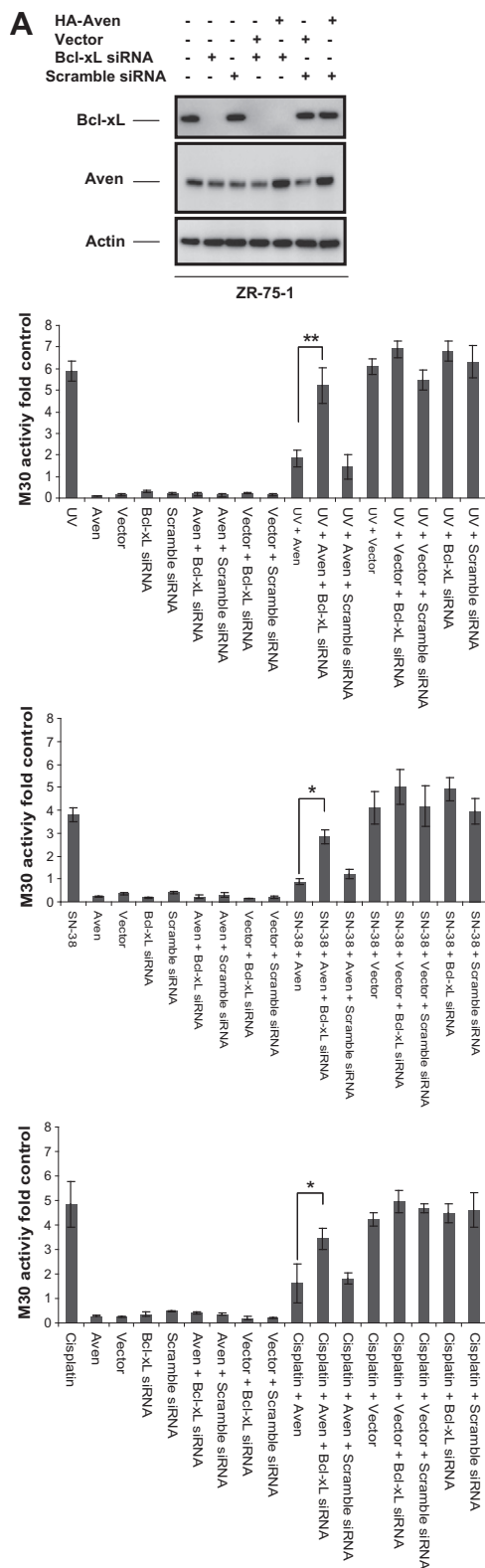
of caspase-3 and caspase-9, but not caspase-8, following treatment with DNA-damaging agents (Figs. S1B, S2B and S3B).

UV-irradiation has been reported to decrease Bcl-xL levels in rat hepatoma cells,[35] basal carcinoma cell lines[36] and fibroblasts,[37] which was required for loss of mitochondrial membrane potential, caspase activation and cell death. Furthermore, decreased expression of Bcl-xL was shown to mediate apoptosis following SN-38 treatment in human mesothelioma cells or camptothecin treatment in fibroblasts and hepatocellular carcinoma cells.[38–40] Importantly, cisplatin treatment resulted in decreased Bcl-xL protein levels in cisplatin-sensitive ovarian carcinoma cells, whereas Bcl-xL levels did not change in cisplatin-resistant cells.[41] A reduction in Bcl-xL levels was also observed in hepatoma cells and renal tubular cells treated with cisplatin, contributing to cell death response to cisplatin.[42,43] Taken together, these studies underscore the involvement of decrease in Bcl-xL protein levels in DNA damage-induced apoptosis. Given the synergistic prosurvival properties of Aven and Bcl-xL,[34] we evaluated the changes of the expression levels of Bcl-xL and Aven in ZR-75-1 and BT549 exposed to UV damage or treated with SN-38 or cisplatin using immunoblot analysis. In Fig. 2A, we demonstrated that both Bcl-xL and Aven protein levels decreased in ZR-75-1 cells following treatment with DNA-damaging agents. The decrease in Bcl-xL protein level could be detected after 12 h of treatment. Consistent with this finding, a similar reciprocal relationship between Aven and Bcl-xL protein levels was described previously.[34] Likewise, Bcl-xL levels were decreased in BT549 cells in response to DNA-damaging treatments. In contrast, we could not detect any alteration in Aven protein levels after treatment with UV, SN-38 or cisplatin in BT549 cells (Fig. 2A). This is interesting, as downregulation of Aven is not always required for Bcl-xL degradation in response to DNA damage. Considering the established interaction of Aven with Bcl-xL,[28] we asked whether treatment with DNA-damaging agents alters the interaction between Aven and Bcl-xL. To address this issue, we exposed ZR-75-1 and BT549 cells to UV damage or treated cells with SN-38 or cisplatin. Total proteins were isolated after 9 h post-treatment and the interaction between Bcl-xL and Aven was evaluated by means of reciprocal coimmunoprecipitation assays. As

◄

Fig. 2 – Aven prevents DNA damage-induced decrease in Bcl-xL protein levels. (A) ZR-75-1 and BT549 cells were exposed to UV (80 mJ/cm^2) or treated with SN-38 (60 nM) and cisplatin (20 μM) for. Cells were lysed at 0–48 h time intervals and cellular extracts were immunoblotted with Bcl-xL or Aven antibody. Actin was probed as an internal loading control. (B) ZR-75-1 and BT549 cells were exposed to UV (80 mJ/cm^2) or treated with SN-38 (60 nM) and cisplatin (20 μM) for 9 h. Total cell lysates were prepared in 1% Chaps buffer and the interaction of Aven with Bcl-xL was evaluated by reciprocal coimmunoprecipitation assays. Input for coimmunoprecipitation was also subjected to immunoblot analysis and actin was probed as a loading control. (C) ZR-75-1 and BT549 cells were transfected either with empty vector (pSG5 Vector) or with pSG5 HA-Aven. Aven-transfected, vector-transfected and untransfected cells were exposed to UV (80 mJ/cm^2) or treated with SN-38 (60 nM) and cisplatin (20 μM). Aven and Bcl-xL protein levels were examined by immunoblot analysis after 16 h of treatment. (D) ZR-75-1, pSG5 HA-Aven-transfected ZR-75-1 (ZR-75-1 Aven), BT549 and pSG5 HA-Aven-transfected BT549 (BT549 Aven) cells were treated with 10 μg/ml cycloheximide (CHX) and Bcl-xL protein levels were detected at 0–16 h by immunoblot analysis. Cells were also transfected with Aven siRNA and Bcl-xL protein levels were detected 0–16 h following cycloheximide (10 μg/ml) treatment. Protein expression levels were semi-quantitatively determined by densitometry and shown as a ratio of Bcl-xL/Actin.

shown in Fig. 2B, Bcl-xL is complexed with Aven in untreated ZR-75-1 and BT549 cells, and treatment with DNA-damaging agents markedly diminished the interaction of Bcl-xL with Aven. Similar results were observed in reciprocal coimmuno-

precipitation experiments using anti-Aven antibody (Fig. 2B). Therefore, it is likely that the disruption of Aven/Bcl-xL complex promotes decreased levels of Bcl-xL by enhancing its degradation. Indeed, the decrease in Bcl-xL protein levels fol-

lowing treatment with DNA-damaging agents was reported to be regulated by the proteasome-mediated protein degradation pathway.[36,39] While the degradation of Bcl-xL in response to camptothecin treatment was blocked by the proteasome inhibitor MG132, pretreatment with the pancaspase inhibitor zVAD-FMK did not show any effect.[39] Thus, the mechanism of Aven-induced prosurvival against DNA-damaging agents may involve the protection of Bcl-xL from degradation. To test this possibility, we examined the effect of Aven overexpression on Bcl-xL protein levels following treatment with UV, cisplatin or SN-38. ZR-75-1 and BT549 cells were transfected either with empty vector or with HA-Aven followed by treatment with UV, cisplatin or SN-38. The protein levels of Bcl-xL and Aven were detected by immunoblot analysis after 16 h post-treatment. Our results demonstrate that overexpression of Aven in ZR-75-1 and BT549 cells prevented DNA damage-induced decrease in Bcl-xL protein levels (Fig. 2C). Transfection with empty vector alone did not alter the Bcl-xL levels in untreated cells or in cells treated with UV, cisplatin or SN-38.

Since overexpression of Aven prevented DNA damage-induced Bcl-xL degradation, we studied the half-life of Bcl-xL in the presence or the absence of enforced Aven expression by using cycloheximide blockade. Our results demonstrate that protein half-life of Bcl-xL was markedly longer in cycloheximide-treated Aven-overexpressing ZR-75-1 and BT549 cells compared with untransfected control cells (Fig. 2D). Correspondingly, knockdown of Aven by means of RNA interference led to shortened Bcl-xL half-life compared with untransfected control cells (Fig. 2D). These results suggest that Aven augments the stability of Bcl-xL, which may explain the protective effect of Aven against DNA damage-induced apoptosis in breast cancer cells. Of note, enforced Aven expression did not affect the stability of Mcl-1 and Bcl-2 proteins (Fig. S5), indicating the specificity of Bcl-xL stabilisation by Aven among antiapoptotic Bcl-2 protein family members. Reasoning that Aven also interacts with Apaf-1 to exert its prosurvival function at the level of apoptosome by preventing its oligomerisation,[28] we next asked whether the protective effect of Aven against DNA damage-induced apoptosis requires the presence of Bcl-xL. To test this hypothesis, we depleted endogenous Bcl-xL by using siRNA-mediated knockdown, which is followed by overexpression of Aven in untreated or siRNA-treated cells. Knockdown of Bcl-xL and enforced expression of Aven in ZR-75-1 and BT549 cells were confirmed by immunoblot analysis (Fig. 3A and B). Cells were exposed to UV or treated with SN-38 or cisplatin and apoptotic responses were evaluated by M30 Apoptosense ELISA assays. As demonstrated in Fig. 3A and B, knockdown of Bcl-xL in ZR-75-1 and BT549 cells resulted in loss of protection by Aven against apoptosis induced by UV, SN-38 or cisplatin

treatment. Annexin V staining assays also confirmed these results (Fig. S6). Treatment with Scrambled siRNA or transfection with empty vector alone did not show any significant effect on apoptotic response. In addition, knockdown of Bcl-xL did not significantly enhance the cell death response by DNA-damaging treatments, which may be due to already activated prodeath signalling promoting Bcl-xL degradation in ZR-75-1 and BT549 cells. Intriguingly, siRNA-mediated depletion of Aven resulted in increased cell death response following treatment with DNA-damaging agents (Fig. 1D). The reason may be that Aven has targets other than Bcl-xL, such as Apaf-1,[28] for its prosurvival function and thereby its knockdown had a more evident effect than Bcl-xL on DNA damage-induced apoptosis. Together, the data demonstrate that Bcl-xL significantly contributes to the prosurvival effect of Aven against DNA damage-induced apoptosis in breast cancer cells.

Consistent with its prosurvival role, Aven was shown to be expressed at a higher level in relapsed patients and to be an independent poor prognostic factor in acute leukaemia.[44,45] To further investigate the role of Aven in breast cancer, we next performed immunohistochemical analysis on two tissue microarrays (TMAs) containing 90 breast cancer specimens (infiltrating ductal carcinoma (n = 69), infiltrating lobular carcinoma (n = 5), papillary carcinoma (n = 12), Phyllodes tumour (n = 4) and 8 non-neoplastic breast tissue specimens. Haematoxylin–eosin staining was carried out to identify representative tumour areas in the TMA sections (Fig. S7). We evaluated the intensity and the distribution of staining using semi-quantitative immunoreactive score (IRS) methodology.[33] Our results showed that immunostaining of Aven could be detected in cytoplasm and nucleus of non-neoplastic breast tissues and breast cancer tissues (Fig. 4A). We could not detect any significant difference in the total or cytoplasmic IRS of Aven between non-neoplastic breast tissues and breast cancer tissues (Fig. 4B). However, Aven nuclear expression was significantly lower in breast cancer tissues compared with non-neoplastic breast tissues. Next, we determined the cytoplasmic and nuclear IRS of Aven in subtypes of breast cancer tissues. Our results demonstrated similar IRS for cytoplasmic expression of Aven in all breast cancer subtypes and non-neoplastic breast tissues, whereas IRS for Aven nuclear expression was significantly lower in infiltrating ductal carcinoma and papillary carcinoma (a variant of ductal carcinoma *in situ*) compared with non-neoplastic breast cancer tissues and infiltrating lobular carcinoma (Fig. 4C and D). The distribution of breast cancer tissues with low (IRS 0-6) and high (IRS 6-12) Aven expression in relation to clinical and pathological characteristics is shown in Table 1. Our findings did not indicate a significant association between

Fig. 3 – Knockdown of Bcl-xL abrogates protection by Aven against DNA damage-induced apoptosis. (A) ZR-75-1 and (B) BT549 cells were treated with Bcl-xL siRNA or scrambled siRNA for 24 h and then transfected with empty vector (pSG5 Vector) or with pSG5 HA-Aven for another 24 h. Total cell lysates were analysed by immunoblot for Bcl-xL and Aven 48 h post-treatment with Bcl-xL or Scrambled siRNA. Actin was probed as a loading control. Cells were then exposed to UV (80 mJ/cm²) or treated with SN-38 (60 nM) and cisplatin (20 μM). Apoptosis was assessed by M30 Apoptosense assay after 48 h (mean ± SEM, n = 4, *p < 0.05, **p < 0.01 by two-tailed t-test).
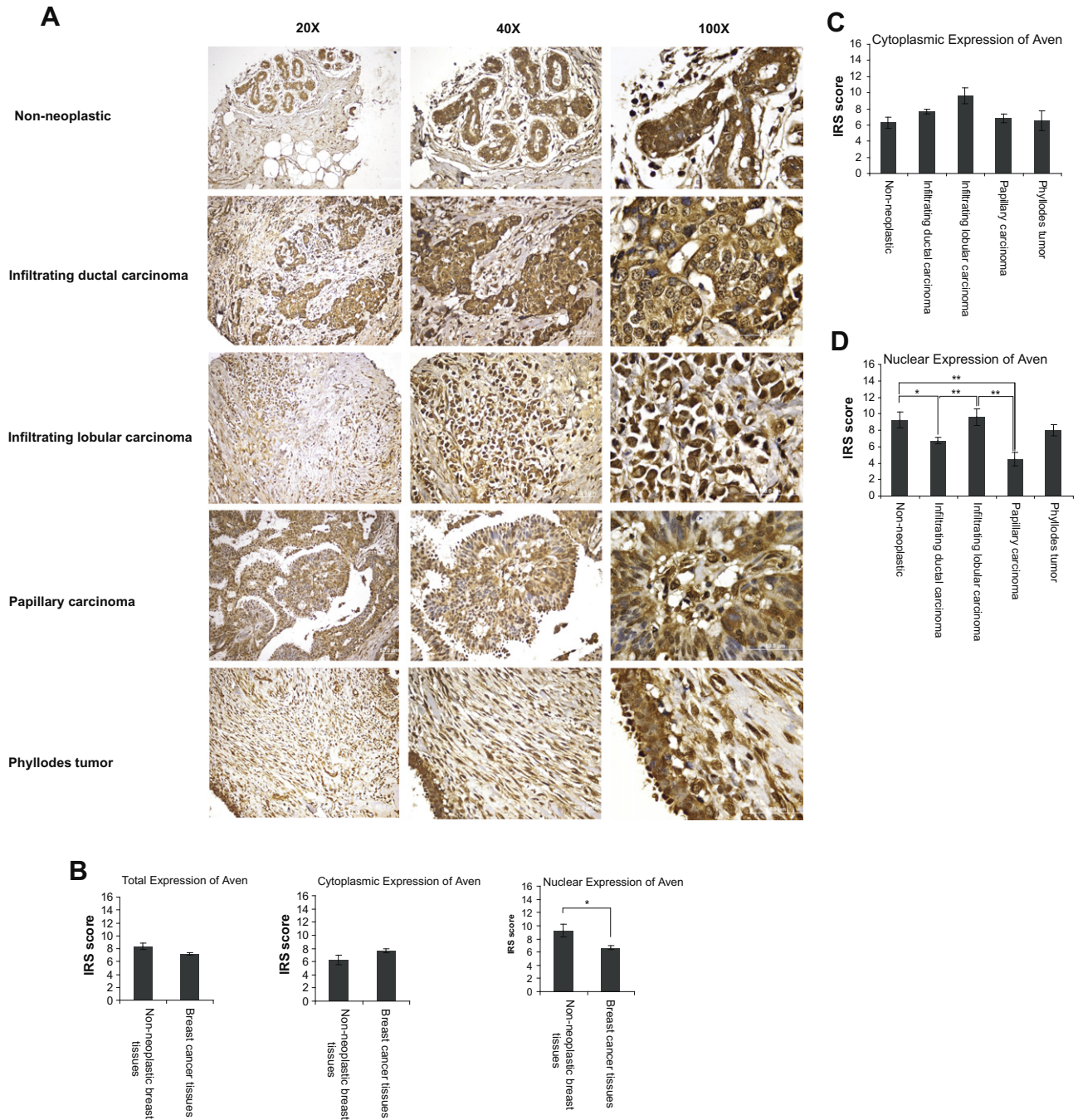
Fig. 4 – Aven protein expression in normal and malignant breast tissues. (A) Representative images of immunohistochemical staining by Aven antibody of human non-neoplastic and breast cancer tissue microarrays (non-neoplastic breast tissue, infiltrating ductal carcinoma, infiltrating lobular carcinoma, papillary carcinoma and Phyllodes tumour). Scale bar represents 50 μm. Magnifications: 20×, 40× and 100×. **(B)** IRS of total, cytoplasmic and nuclear expression of Aven in non-neoplastic breast tissues and breast cancer tissues were determined in the TMA sections. The mean immunoreactivity scores were as follows: total Aven expression in non-neoplastic tissues, IRS = 8.375 ± 0.532; total Aven expression in breast cancer tissues, IRS = 7.189 ± 0.234; cytoplasmic Aven expression in non-neoplastic tissues, IRS = 6.25 ± 0.700; cytoplasmic Aven expression in breast cancer tissues, IRS = 7.624 ± 0.263; nuclear Aven expression in non-neoplastic tissues, IRS = 9.25 ± 0.977; nuclear Aven expression in breast cancer tissues, IRS = 6.666 ± 0.335. Mann–Whitney U test was used for comparison of data; significance was set at $*p < 0.05$. IRS for **(C)** cytoplasmic and **(D)** nuclear expression of Aven in non-neoplastic tissues and subtypes of breast cancer tissues are shown here. Aven immunohistochemical staining was detectable in both cytoplasm and nucleus of benign and malignant breast tissues. Nevertheless, nuclear expression of Aven in infiltrating ductal carcinoma and papillary carcinoma was significantly less abundant compared with that in non-neoplastic breast cancer tissues. Mann–Whitney U test was used for comparison of data. Differences were considered significant when $*p < 0.05$ and $**p < 0.01$.

Table 1 – Clinical and pathological parameters of cases included in tissue microarrays are summarized (described according to American Joint Committee on Cancer (AJCC) TNM system). Breast cancer tissue sections were divided into low Aven expressing (IRS 0-6) and high Aven expressing (IRS 6-12) groups. SPSS/PC software package version 13.0 (SPPS, Chicago, USA) was used for statistical data analysis. Kruskal–Wallis test was used to evaluate the association between clinical and pathological parameters and low/high Aven expression. Significance was set at *p < 0.05 (1, p value for low Aven expressing cases; 2, p value for high Aven expressing cases). Abbreviations: pN, lymph node status; pT, tumor size and invasion; IRS, immunoreactive score; ER, estrogen receptor; PR, progesterone receptor.

Characteristics		Low Aven (score–6)	High Aven (score 6–12)	Total n (%)	p-Value (1,2)
Association of Aven immunoreactivity with clinical and pathological characteristics					
Total					
Age	<50	18 (32.7)	37 (66.3)	55(100)	0.961, 0.045*
	50–59	2 (18.2)	9 (81.8)	11 (100)	
	60–69	7 (43.7)	9 (56.3)	16 (100)	
	>70	5 (62.5)	3 (37.5)	8 (100)	
	Total	32 (35.5)	58 (64.5)	90 (100)	
pT	pT1	10 (34.5)	19 (65.5)	29 (100)	0.223, 0.483
	pT2–4	19 (37.2)	32 (62.8)	51 (100)	
	Total	29 (35.8)	51 (64.2)	80 (100)	
pN	pN0	21(48.8)	22 (51.2)	43 (100)	0.478, 0.999
	pN1	6 (28.6)	15 (71.4)	21 (100)	
	pN2	1 (12.5)	7 (87.5)	8 (100)	
	pN3	2 (22.2)	7 (77.8)	9 (100)	
	Total	30 (37)	51 (63)	81(100)	
Grading	1 or 2	18 (36.7)	31 (63.3)	49 (100)	0.221, 0.776
	3 or 4	11 (35.5)	20 (64.5)	31 (100)	
	Total	29 (36.2)	51 (63.8)	80 (100)	
ER status	Negative	10 (50)	10 (50)	20 (100)	0.506, 0.781
	Positive	21 (33.9)	41 (66.1)	62 (100)	
	Total	31 (37.8)	51 (62.2)	82 (100)	
PR status	Negative	12 (44.4)	15 (55.6)	27 (100)	0.883, 0.965
	Positive	19 (35.2)	35 (64.8)	54 (100)	
	Total	31 (38.3)	50 (61.7)	81 (100)	
c-erB-2 status	Negative	19 (38.8)	30 (61.2)	49 (100)	0.582, 0.765
	Positive	20 (64.5)	11 (33.5)	31 (100)	
	Total	39 (48.7)	41 (51.3)	80 (100)	

low or high expression of Aven and pT, pN, grade, ER status, PR status and c-erB-2 status. In fact, there was a significant association between total Aven expression and age, as decreased total Aven expression was detected with increasing age (Table 1). Defective DNA damage response, including failed cell cycle checkpoints and DNA repair machinery, promotes the generation of genomic instability in cancer cells. It is noted that genomic instability potentially drives tumourigenesis in invasive breast carcinomas by promoting the acquisition of specific gene alterations. Chromosome instability was reported in nearly 70% of breast tumours by deletions, amplifications, rearrangements and aneuploidy.[46] In particular, infiltrating ductal breast cancers are characterised by increased chromosomal instability compared with infiltrating lobular breast cancers.[47] ATM has been proposed as a susceptibility gene in sporadic breast cancer.[48,49] Hence, ATM protein levels were found to be lower in sporadic invasive ductal breast carcinomas[50] and a significant reduction in the intensity of the nuclear ATM staining in epithelial cancer cells was detected in 59% of breast tumours examined.[51] Considering that Aven directly regulates ATM function in response to DNA damage,[29] decreased Aven nuclear expression might contribute to higher chromosome instability in breast cancer tumours. Thus, our findings undercover a novel mechanism for the prosurvival function of Aven in breast cancer cells and identify Aven as a candidate protein regulating DNA damage response in human breast cancer.

Conflict of interest statement

None declared.

Acknowledgements

Appendix A. Supplementary data

Supplementary data associated with this article can be found, in the online version, at doi:10.1016/j.ejca.2010.06.011.

REFERENCES

1. Roos WP, Kaina B. DNA damage-induced cell death by apoptosis. *Trends Mol Med* 2006;**12**:440–50.
2. Norbury CJ, Zhivotovsky B. DNA damage-induced apoptosis. *Oncogene* 2004;**23**:2797–808.
3. Westphal CH, Rowan S, Schmaltz C, et al. Atm and p53 cooperate in apoptosis and suppression of tumorigenesis, but not in resistance to acute radiation toxicity. *Nat Genet* 1997;**16**:397–401.
4. Cheung AM, Elia A, Tsao MS, et al. Brca2 deficiency does not impair mammary epithelium development but promotes mammary adenocarcinoma formation in p53(+/−) mutant mice. *Cancer Res* 2004;**64**:1959–65.
5. Boehrer S, Ades L, Tajeddine N, et al. Suppression of the DNA damage response in acute myeloid leukemia versus myelodysplastic syndrome. *Oncogene* 2009;**28**:2205–18.
6. Bedi A, Barber JP, Bedi GC, et al. BCR-ABL-mediated inhibition of apoptosis with delay of G2/M transition after DNA damage: a mechanism of resistance to multiple anticancer agents. *Blood* 1995;**86**:1148–58.
7. Gewirtz DA. Growth arrest and cell death in the breast tumor cell in response to ionizing radiation and chemotherapeutic agents which induce DNA damage. *Breast Cancer Res Treat* 2000;**62**:223–35.
8. Runger TM, Emmert S, Schadendorf D, et al. Alterations of DNA repair in melanoma cell lines resistant to cisplatin, fotemustine, or etoposide. *J Invest Dermatol* 2000;**114**:34–9.
9. Hodkinson PS, Elliott T, Wong WS, et al. ECM overrides DNA damage-induced cell cycle arrest and apoptosis in small-cell lung cancer cells through beta1 integrin-dependent activation of PI3-kinase. *Cell Death Differ* 2006;**13**:1776–88.
10. Ekert PG, Jabbour AM, Manoharan A, et al. Cell death provoked by loss of interleukin-3 signaling is independent of Bad, Bim, and PI3 kinase, but depends in part on Puma. *Blood* 2006;**108**:1461–8.
11. Brunelle JK, Shroff EH, Perlman H, et al. Loss of Mcl-1 protein and inhibition of electron transport chain together induce anoxic cell death. *Mol Cell Biol* 2007;**27**:1222–35.
12. Wang GQ, Gastman BR, Wieckowski E, et al. A role for mitochondrial Bak in apoptotic response to anticancer drugs. *J Biol Chem* 2001;**276**:34307–17.
13. Mandic A, Viktorsson K, Molin M, et al. Cisplatin induces the proapoptotic conformation of Bak in a deltaMEKK1-dependent manner. *Mol Cell Biol* 2001;**21**:3684–91.
14. Dunkern TR, Fritz G, Kaina B. Ultraviolet light-induced DNA damage triggers apoptosis in nucleotide excision repair-deficient cells via Bcl-2 decline and caspase-3/-8 activation. *Oncogene* 2001;**20**:6026–38.
15. Zou H, Li Y, Liu X, Wang X. An APAF-1.cytochrome c multimeric complex is a functional apoptosome that activates procaspase-9. *J Biol Chem* 1999;**274**:11549–56.
16. Certo M, Del Gaizo Moore V, Nishino M, et al. Mitochondria primed by death signals determine cellular addiction to antiapoptotic BCL-2 family members. *Cancer Cell* 2006;**9**:351–65.
17. Letai A, Bassik MC, Walensky LD, et al. Distinct BH3 domains either sensitize or activate mitochondrial apoptosis, serving as prototype cancer therapeutics. *Cancer Cell* 2002;**2**:183–92.
18. Chen L, Willis SN, Wei A, et al. Differential targeting of prosurvival Bcl-2 proteins by their BH3-only ligands allows complementary apoptotic function. *Mol Cell* 2005;**17**:393–403.
19. Willis SN, Chen L, Dewson G, et al. Proapoptotic Bak is sequestered by Mcl-1 and Bcl-xL, but not Bcl-2, until displaced by BH3-only proteins. *Genes Dev* 2005;**19**:1294–305.
20. Kohl TM, Hellinger C, Ahmed F, et al. BH3 mimetic ABT-737 neutralizes resistance to FLT3 inhibitor treatment mediated by FLT3-independent expression of BCL2 in primary AML blasts. *Leukemia* 2007;**21**:1763–72.
21. Kuroda J, Kimura S, Andreeff M, et al. ABT-737 is a useful component of combinatory chemotherapies for chronic myeloid leukaemias with diverse drug-resistance mechanisms. *Br J Haematol* 2008;**140**:181–90.
22. Kutuk O, Letai A. Alteration of the mitochondrial apoptotic pathway is key to acquired paclitaxel resistance and can be reversed by ABT-737. *Cancer Res* 2008;**68**:7985–94.
23. Ding Q, He X, Xia W, et al. Myeloid cell leukemia-1 inversely correlates with glycogen synthase kinase-3beta activity and associates with poor prognosis in human breast cancer. *Cancer Res* 2007;**67**:4564–71.
24. Buchholz TA, Davis DW, McConkey DJ, et al. Chemotherapy-induced apoptosis and Bcl-2 levels correlate with breast cancer response to chemotherapy. *Cancer J* 2003;**9**:33–41.
25. Bourguignon LY, Xia W, Wong G. Hyaluronan-mediated CD44 interaction with p300 and SIRT1 regulates beta-catenin signaling and NFkappaB-specific transcription activity leading to MDR1 and Bcl-xL gene expression and chemoresistance in breast tumor cells. *J Biol Chem* 2009;**284**:2657–71.
26. Olopade OI, Adeyanju MO, Safa AR, et al. Overexpression of BCL-x protein in primary breast cancer is associated with high tumor grade and nodal metastases. *Cancer J Sci Am* 1997;**3**:230–7.
27. Amundson SA, Myers TG, Scudiero D, et al. An informatics approach identifying markers of chemosensitivity in human cancer cell lines. *Cancer Res* 2000;**60**:6101–10.
28. Chau BN, Cheng EH, Kerr DA, Hardwick JM. Aven, a novel inhibitor of caspase activation, binds Bcl-xL and Apaf-1. *Mol Cell* 2000;**6**:31–40.
29. Guo JY, Yamada A, Kajino T, et al. Aven-dependent activation of ATM following DNA damage. *Curr Biol* 2008;**18**:933–42.
30. Hagg M, Biven K, Ueno T, et al. A novel high-through-put assay for screening of pro-apoptotic drugs. *Invest New Drugs* 2002;**20**:253–9.
31. Leu JI, Dumont P, Hafey M, Murphy ME, George DL. Mitochondrial p53 activates Bak and causes disruption of a Bak-Mcl1 complex. *Nat Cell Biol* 2004;**6**:443–50.
32. Panaretakis T, Pokrovskaja K, Shoshan MC, Grander D. Activation of Bak, Bax, and BH3-only proteins in the apoptotic response to doxorubicin. *J Biol Chem* 2002;**277**:44317–26.
33. Remmele W, Stegner HE. Recommendation for uniform definition of an immunoreactive score (IRS) for immunohistochemical estrogen receptor detection (ER-ICA) in breast cancer tissue. *Pathologe* 1987;**8**:138–40.
34. Figueroa Jr B, Chen S, Oyler GA, Hardwick JM, Betenbaugh MJ. Aven and Bcl-xL enhance protection against apoptosis for mammalian cells exposed to various culture conditions. *Biotechnol Bioeng* 2004;**85**:589–600.
35. Scoltock AB, Heimlich G, Cidlowski JA. Glucocorticoids inhibit the apoptotic actions of UV-C but not Fas ligand in hepatoma cells: direct evidence for a critical role of Bcl-xL. *Cell Death Differ* 2007;**14**:840–50.
36. Park K, Lee JH. Bcl-XL protein is markedly decreased in UVB-irradiated basal cell carcinoma cell lines through proteasome-mediated degradation. *Oncol Rep* 2009;**21**:689–92.
37. Nakagawa Y, Okada S, Hatano M, et al. Downregulation of bcl-xL is relevant to UV-induced apoptosis in fibroblasts. *J Biochem Mol Biol* 2002;**35**:452–8.
38. Russo P, Catassi A, Malacarne D, et al. Tumor necrosis factor enhances SN38-mediated apoptosis in mesothelioma cells. *Cancer* 2005;**103**:1503–18.
39. Tomicic MT, Christmann M, Kaina B. Topotecan triggers apoptosis in p53-deficient cells by forcing degradation of XIAP and survivin thereby activating caspase-3 mediated Bid cleavage. *J Pharmacol Exp Ther* 2010;**332**:316–25.

40. Takeba Y, Kumai T, Matsumoto N, et al. Irinotecan activates p53 with its active metabolite, resulting in human hepatocellular carcinoma apoptosis. *J Pharmacol Sci* 2007;**104**:232–42.

41. Villedieu M, Louis MH, Dutoit S, et al. Absence of Bcl-xL down-regulation in response to cisplatin is associated with chemoresistance in ovarian carcinoma cells. *Gynecol Oncol* 2007;**105**:31–44.

42. Qin LF, Ng IO. Induction of apoptosis by cisplatin and its effect on cell cycle-related proteins and cell cycle changes in hepatoma cells. *Cancer Lett* 2002;**175**:27–38.

43. Jiang M, Wei Q, Wang J, et al. Regulation of PUMA-alpha by p53 in cisplatin-induced renal cell apoptosis. *Oncogene* 2006;**25**:4056–66.

44. Paydas S, Tanriverdi K, Yavuz S, et al. Survivin and aven: two distinct antiapoptotic signals in acute leukemias. *Ann Oncol* 2003;**14**:1045–50.

45. Choi J, Hwang YK, Sung KW, et al. Aven overexpression: association with poor prognosis in childhood acute lymphoblastic leukemia. *Leuk Res* 2006;**30**:1019–25.

46. Huiping C, Johannsdottir JT, Arason A, et al. Replication error in human breast cancer: comparison with clinical variables and family history of cancer. *Oncol Rep* 1999;**6**:117–22.

47. Huiping C, Sigurgeirsdottir JR, Jonasson JG, et al. Chromosome alterations and E-cadherin gene mutations in human lobular breast cancer. *Br J Cancer* 1999;**81**:1103–10.

48. Broeks A, Urbanus JH, Floore AN, et al. ATM-heterozygous germline mutations contribute to breast cancer-susceptibility. *Am J Hum Genet* 2000;**66**:494–500.

49. Vo QN, Kim WJ, Cvitanovic L, et al. The ATM gene is a target for epigenetic silencing in locally advanced breast cancer. *Oncogene* 2004;**23**:9432–7.

50. Kairouz R, Clarke RA, Marr PJ, et al. ATM protein synthesis patterns in sporadic breast cancer. *Mol Pathol* 1999;**52**:252–6.

51. Angele S, Treilleux I, Taniere P, et al. Abnormal expression of the ATM and TP53 genes in sporadic breast carcinomas. *Clin Cancer Res* 2000;**6**:3536–44.